ACS OMEGA

Open Access

http://pubs.acs.org/journal/acsodf

Article

Single Ni Atom-Dispersed WSe_2 Monolayer for Sensing Typical Fault Gases in Dry-Type Transformers: A First-Principles Study

Yan Liu, Jianben Liu, Zhuo Wei, Tian Yuan, and Hao Cui*

Cite This: *ACS Omega* 2023, 8, 47067−47074

Read Online

ACCESS | Metrics & More | Article Recommendations

ABSTRACT: This work, using the first-principles theory, uses the Ni-decorated WSe_2 (Ni-WSe_2) monolayer as a novel gas sensing material upon CO and HCHO in the dry-type transformers in order to evaluate their operation status. Results indicate that the Ni atom can be stably adsorbed on the T_W site of the pristine WSe_2 monolayer with the binding force of −4.33 eV. Via the gas adsorption analysis, it is found that the Ni-WSe_2 monolayer performs chemisorption upon CO and HCHO molecules, with adsorption energies of −2.27 and −1.37 eV, respectively. The analyses of the band structure and Frontier molecular orbital manifest the potential of the Ni-WSe_2 monolayer as a resistance-type gas sensor upon CO and HCHO, with sensing responses of 55.9 and 30.9% based on the band gap change and of 55.0 and 38.5% based on the energy gap change. The analysis of the density of state clearly shows the modified electronic property of the Ni-WSe_2 monolayer in gas adsorptions. On the other hand, the analysis of the work function (WF) reveals the limited possibility to explore the Ni-WSe_2 monolayer as a WF-based gas sensor for CO and HCHO detections. This work systemically studies the sensing potential of the Ni-WSe_2 monolayer upon two typical gas species in the dry-type transformers, which is meaningful to explore novel nanomaterial-based gas sensors to monitor the operation condition of electrical equipment.

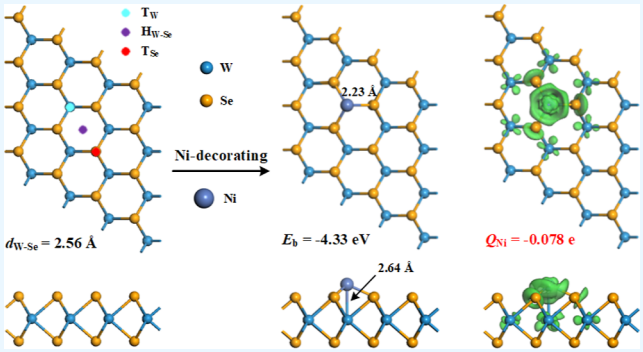

1. INTRODUCTION

In the power system, dry-type transformers account for over 40% of application for electricity transmissions and distributions in some typical environment, such as urban load centers and building indoor power distribution.[1] To guarantee the good insulation performance of dry-type transformers, epoxy resin is selected as the insulation media, and in the epoxy resin, some additives are applied to promotes its fire resistance and arc extinction behaviors.[2,3] However, the insulation performance of the epoxy resin would be weakened in long-term running, and it cannot undergo the perennial defects including partial overheat and discharge. Therefore, the epoxy resin would be decomposed into several toxic gas species,[4] such as CO and HCHO.[5] On the one hand, these gases can be used to reflect the working operation of the dry-type-transformer;[6] on the other hand, these gases would be pervaded in the transformer substation which would pose great threats to the maintenance persons. In these regards, the sensing of CO and HCHO around the dry-type transformers is quite significant and meaningful for the safety for the power system and human health.[7]

For the purpose of gas sensing, the nanomaterial-based gas sensors are dramatically developed in recent decades, and the novel sensing materials with low cost, rapid response, and high sensitivity are largely explored in this field.[8−12] Recently, the transition metal dichalcogenides (TMDs) with two-dimensional structure are tremendously investigated for gas sensing application,[13−15] due to their admirable structural properties and tunable semiconducting behaviors.[16,17] For instance, the MoS_2 and $MoSe_2$ monolayer are widely explored from theoretical and experimental aspects for toxic gas sensing in some typical and harsh environments.[18−21] Also, the WS_2 and WSe_2 monolayers are studied in terms of their electronic properties and gas sensing performance.[21,22] When it comes to the WSe_2 monolayer, the transition metal decorated counterpart are reported with a desirable sensing performance, in which the Pd and Pt adatoms can largely promote the binding strength and charge transfer between the WSe_2 surface and gas molecules (including CO and SF_6 decomposed species[23,24]). These reports indicate the strong potential to explore the WSe_2-based gas sensor for CO and HCHO sensing in the dry-type transformers.

Received: September 12, 2023
Revised: October 8, 2023
Accepted: November 3, 2023
Published: November 27, 2023

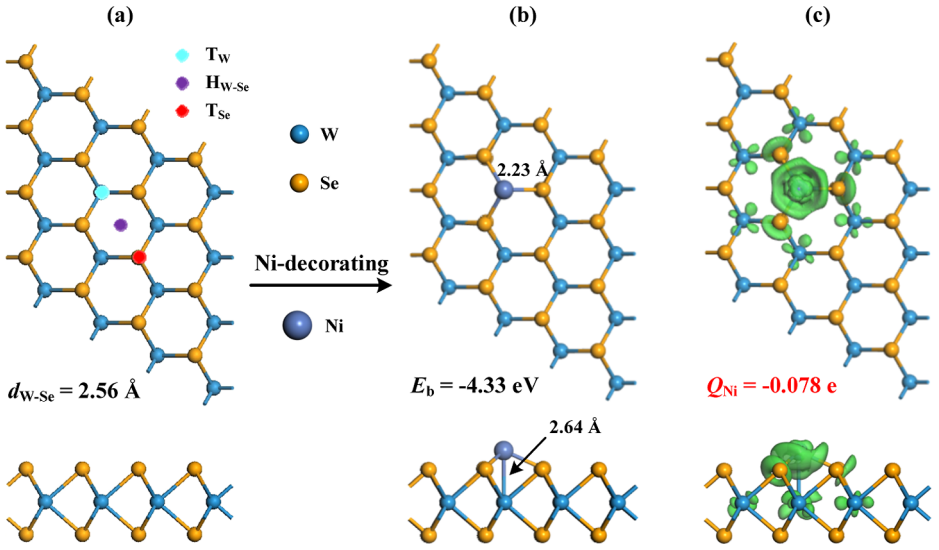

Figure 1. Ni-decorating behavior on the WSe_2 monolayer (a) pristine WSe_2 monolayer, (b,c) morphology and related CDD of the Ni-WSe_2 monolayer. In CDD, the green area is the electron accumulation, and the isosurface is set at 0.01 e/Å^3.

Within the same group of Pd and Pt atoms, the Ni atom is also widely applied for surface-decoration on the nanomaterials to explore their sensing potentials.[25−27] Therefore, we presume that the Ni-decorated WSe_2 (Ni-WSe_2) monolayer can perform comparable adsorption and sensing properties upon gas species to the previous reports regarding Pd- or Pt-decorated counterparts. Besides, such an investigation would be significant to uncover such performances of the Ni-WSe_2 monolayer and broaden the application domains for the WSe_2 monolayer. In this work, we systemically use the first-principles theory to illustrate the Ni-decorating property on the pristine WSe_2 surface and the adsorption and sensing mechanisms of Ni-WSe_2 monolayer upon CO and HCHO and eventually explore its potential as a gas sensor to evaluate the running status of the dry-type transformers (Section 3). Apart from those, Section 2 gives the computational details, while Section 4 gives the main conclusions.

2. COMPUTATIONAL DETAILS

The whole theoretical calculations were all based on the first-principles theory and conducted within the DMol^3 code.[28,29] We employed the Perdew−Burke−Ernzerhof function to deal with the electron exchange and correlation terms[30] and adopted the DFT-D2 method, raised by Tkatchenko and Scheffler, to cope with the van der Waals force and the long-range interactions.[31] The double numerical plus polarization was selected as the basis set for the atomic orbital, while the DFT semicore pseudo potential (DSSP) method was defined to resolve the relativistic effect of the Ni dopant.[32] The *k*-point of 10 × 10 × 1 was sampled in the Brillouin zone for geometric and electronic calculations.[33] Besides, the self-consistent loop energy of 10^{-6} Ha, global orbital cutoff radius of 5.0 Å and smearing of 0.005 Ha were determined to guarantee the good accuracy of the total energies in each system.[34] One should note that all of the simulations were performed under 0 K and a vacuum region.

The pristine WSe_2 monolayer was established, and the supercell lattice is enlarged to be 4 × 4, including 16 W atoms and 32 Se atoms. Also, a 20 Å vacuum region was defined to prevent possible interaction among adjacent units.[35] The binding energy (E_b) was defined to evaluate the binding force between the Ni atom and the intrinsic WSe_2 surface, calculated by[36]

$$E_b = E_{\text{Ni-WSe}_2} - E_{\text{WSe}_2} - E_{\text{Ni}} \quad (1)$$

where $E_{\text{Ni-WSe}_2}$ and E_{WSe_2} signified the total energies of the Ni-decorated and intrinsic WSe_2 monolayer, respectively, while E_{Ni} indicated the energy of the single Ni atom in its bulk structure. For CO and HCHO adsorptions on the Ni-WSe_2 monolayer, the adsorption energy (E_{ad}) was defined to evaluate the binding strength of the Ni-WSe_2 surface upon two gas species, calculated by[37]

$$E_{ad} = E_{\text{Ni-WSe}_2/\text{gas}} - E_{\text{Ni-WSe}_2} - E_{\text{gas}} \quad (2)$$

where $E_{\text{Ni-WSe}_2/\text{gas}}$ and E_{gas} were the total energy of the Ni-WSe_2/gas system and isolated Ni-WSe_2 system, respectively. Moreover, we applied Hirshfeld analysis to analyze the atomic charge of the Ni adatom (Q_{Ni}) in the Ni-WSe_2 system and charge transfer (Q_T) in the gas adsorbed systems. On basis of such definition, a positive value indicated the electron-donating property of the Ni adatom or the gas species.

3. RESULTS AND DISCUSSION

3.1. Ni-Decorating Behavior on the Pristine WSe_2 Monolayer. For Ni-decorating on the pristine WSe_2 surface, we consider three possible sites, traced as the T_W site (on the top of the W atom), H_{W-Se} site (on the top of the hollow W−Se ring), and the T_{Se} site (on the top of the Se atom) for single Ni atom adsorption on the WSe_2 monolayer. By such a definition, the dispersing concentration is calculated as 2.08%. The Ni-decorating process, including the morphology and defined decorating site of the pristine WSe_2 monolayer, as well as the most preferred morphology with related charge density difference (CDD) of the Ni-WSe_2 monolayer, are exhibited in Figure 1.

First, focusing on the optimized geometry of the pristine WSe_2 monolayer in Figure 1a, we find that the W−Se bond length is 2.56 Å and the lattice constant is 3.34 Å, which are consistent with the previous findings of 2.55 Å for the W−Se bond and 3.32 Å for the lattice constant in ref 22. Then, highlighting the optimized Ni-WSe_2 monolayer in Figure 1b,

https://doi.org/10.1021/acsomega.3c06980
ACS Omega 2023, 8, 47067−47074

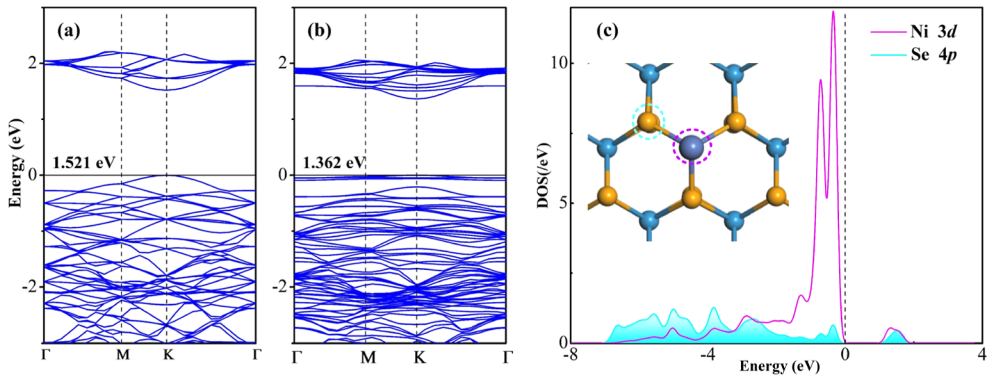

Figure 2. (a,b) BS of intrinsic and Ni-decorated WSe_2 systems, and (c) orbital DOS of the Ni and W and Se atoms. In BS, the black values are the band gaps, and in DOS the Fermi level is set to 0.

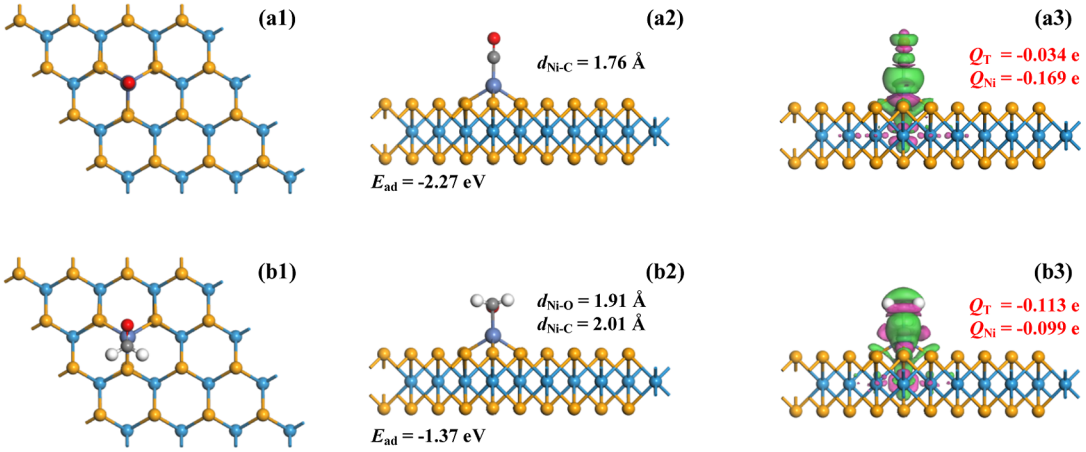

Figure 3. MSC and CDD of the CO (a1−a3) and HCHO (b1−b3) systems. In CDD, the green areas are electron accumulation, while the violet areas are electron depletion, with the isosurface of 0.1 e/Å^3.

one can see that the Ni atom prefers to be adsorbed on the T_W site of the intrinsic WSe_2 monolayer; the Ni adatom is bonded with three Se atoms and one W atom, forming three Ni−Se bonds with equivalent lengths of 2.33 Å and one Ni−W bond with lengths of 2.64 Å. We should note that the Ni−Se bond length is even shorter than summed covalent radii of Ni and Se atoms (2.26 Å[38]), which suggests the strong binding force of the Ni−Se bonds.[39] In contrast, the binding force in the Ni−W bond would be much fainter in comparison with the Ni−Se bonds. According to eq 1, the E_b for Ni-decorating on the intrinsic WSe_2 monolayer is calculated as −4.33 eV, which indicates not only the exothermicity and spontaneity of such a process but also the strong interaction between the Ni atom and the WSe_2 surface.[40] Such a binding force is much more negative than that of the T_{Se} site of −3.77 eV and that of the H_{W-Se} site of −3.49 eV. Moreover, the vibrational analysis is conducted to verify the good chemical stability of the preferred Ni-WSe_2 configuration, and the results show that the frequencies of the Ni-WSe_2 monolayer are ranging at 69.08−741.30 cm^{-1}, which without the imaginary frequency indicating our positive assumption. When it comes to the CDD of the Ni-WSe_2 monolayer in Figure 1c, one can see that the electron accumulations are mainly located on the Ni adatom and the Ni−Se bonds. Such electron accumulation on the Ni adatom agrees with the Hirshfeld analysis which shows the electron-accepting property of the Ni adatom with charged value of −0.078 e, and the electron accumulations on the Ni−Se bonds confirm the strong binding force on the Ni−Se bonds on which strong electron accumulation occurs that gives rise to the negative E_b due to the desirable Ni−Se binding force.

To understand the tuned electronic property upon the pristine WSe_2 monolayer by Ni-decorating, we plot the band structure (BS) of the pristine and Ni-decorated WSe_2 systems, as well as the orbital density of state (DOS) of the bonded atoms in Figure 2. It should be noted that there is no magnetic moment for the pristine and Ni-decorated system; therefore, the spin up and spin down are symmetric; therefore, we only plot the spin up for the BS and DOS distributions. For the BS of the pristine WSe_2 monolayer in Figure 2a, one can see that the band gap of the intrinsic WSe_2 monolayer is obtained as 1.521 eV, and the maximum valence band and the minimum conduction band are both located at the *K* point. These findings are in good accordance with ref 41 in which the direct semiconducting property of the pristine WSe_2 monolayer is verified with the band gap of 1.49 eV. Figure 2b plots the BS of the Ni-WSe_2 monolayer, it is seen that the band gap is slightly narrowed to 1.362 eV, and the state density becomes much denser in comparison with the pristine WSe_2 system. These findings manifest the state activation by the Ni-decorating on the WSe_2 system that brings about several novel states for the whole system.[42] Furthermore, analyzing the orbital DOS in Figure 2c, we can see that the Ni 3*d* orbital is strongly overlapped with the Se 4p orbital at −7.0−0 and 1.3−1.8 eV. These state hybridizations reveal the strong orbital interaction

https://doi.org/10.1021/acsomega.3c06980
ACS Omega 2023, 8, 47067−47074

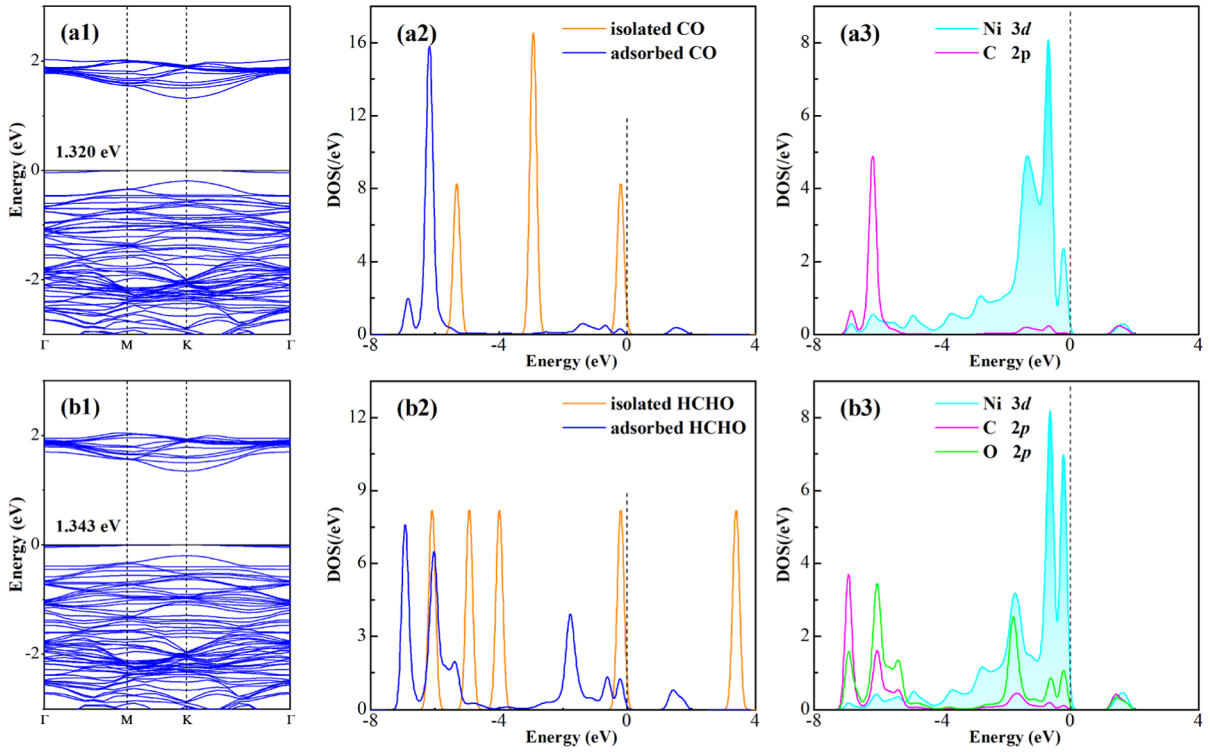

Figure 4. BS and DOS of the CO (a1−a3) and HCHO system (b1−b3). The sets are the same as those in Figure 2.

between the Ni and Se atoms, further confirming the strong binding force on the Ni−Se bonds.

3.2. Adsorption Configuration of Ni-WSe_2/Gas Systems. The optimized Ni-WSe_2 monolayer is determined as the nanosubstrate to conduct the adsorptions upon CO and HCHO molecules, which are put approaching over the Ni adatom with initial distance of about 2.5 Å. Then, we select the configuration with the most negative E_{ad} as the most stable configuration (MSC) for further analyses of geometric and electronic properties. The MSC with related CDD for the CO and HCHO systems is presented in Figure 3. Besides, from the vibrational analysis, the frequencies of the CO and HCHO systems are at 66.45−2187.11 and 68.67−3922.01 cm^{-1}, respectively. One can see that there has no imaginary frequency in such two systems suggesting the good chemical stability of the determined MSC.

For CO adsorption on the Ni-WSe_2 monolayer, one can find that the CO molecule is vertical to the WSe_2 monolayer over the Ni adatom through the C-end position, forming a Ni−C bond that is measured as 1.76 Å. Similarly, we find that such bond length is shorter than the summed covalent radii of the Ni and C atoms (1.85 Å[38]), which could attribute to the strong binding force between Ni adatom and C atom in the CO adsorption process. Apart from that, the average Ni−Se bond length is prolonged to be 2.30 Å from that of 2.23 Å in the pure Ni-WSe_2 system, indicating its geometric distortion upon CO adsorption.[43] Accordingly, the E_{ad} herein is obtained as −2.27 eV, which is much more negative than the critical value of −0.8 eV for the identification of chemisorption in the gas interactions.[44] These findings all manifest the desirable adsorption performance of the Ni-WSe_2 monolayer upon a CO molecule. From the Hirshfeld analysis, the Ni adatom is negatively charged by 0.169 e while the CO molecule is negatively charged by 0.034 e. Combined with the negatively charged value of 0.078 e of the Ni adatom in the isolated Ni-WSe_2 monolayer, we can infer that in the CO adsorption system, the Ni adatom accepts 0.091 e, the CO molecule as a whole accepts 0.034 e, while the WSe_2 surface loses 0.125 e. It should be noted that the majority of the electrons are donated by three Se atoms of the WSe_2 monolayer, which behave as the electron donators in the CO adsorption systems, in which the three Se atoms bonded with the Ni atom donate 0.045 e in total. These findings reveal the strong electron-accepting property in CO adsorption. In other words, the Ni adatom is an electron center that enriches the electron from the WSe_2 monolayer. In the CDD distribution, the electron accumulations are fully surrounded on the Ni adatom, the CO molecule, and the Ni−C bonds, while the electron depletions are surrounded on the C−O bond of the CO molecule and the Ni−Se bond of the Ni-WSe_2 monolayer. These findings not only agree with the Hirshfeld analysis about electron-distribution but also reveal the weakened C−O and Ni−Se bonds in the gas adsorption as well as the formation of Ni−C bonds due to the strong binding force.

Regarding HCHO adsorption on the Ni-WSe_2 monolayer, we can see that the HCHO molecule is almost parallel to the WSe_2 monolayer, in which the O and C atoms are both captured by the Ni adatom, forming the Ni−O and Ni−C bonds with lengths of 1.91 and 2.01 Å, separately. These results show that the Ni adatom has stronger binding force with the O atom compared with the C atom in the HCHO molecule. In other word, the O atom seems to have stronger chemical reactivity in comparison with the C atom in the HCHO molecule. On the other hand, the Ni−C and Ni−O bond lengths are both longer than the summed covalent radii of the Ni and O or C atoms (Ni−O: 1.74 Å, Ni−C: 1.85 Å[38]). From this aspect, one can assume that the Ni-WSe_2 monolayer behaves with relatively weaker performance upon HCHO adsorption compared with CO adsorption. Such ann assumption can also be confirmed by the value of the E_{ad} in

https://doi.org/10.1021/acsomega.3c06980
ACS Omega 2023, 8, 47067−47074

the HCHO system, whose value of −1.37 eV is not as negative as that in the CO system, indicating the weaker gas interaction here. On the other hand, such E_{ad} is still more negative than the critical value of −0.80 eV; thereby, the HCHO adsorption system can also be determined as chemisorption. On basis of the Hirshfeld analysis, the Ni adatom is negatively charged by 0.099 e, while the Q_T is obtained as −0.113 e. In other words, the WSe_2 monolayer loses 0.134 e in the HCHO adsorption, in which the Ni adatom accepts 0.021 e, while the HCHO molecule accepts 0.113 e. Similarly, the Se atoms in the WSe_2 monolayer behave as the electron donators, and the ones bonded with the Ni atoms donate 0.066 e, playing the dominant role for the released electron in the WSe_2 monolayer. These findings reveal the stronger electron-accepting property of the HCHO molecule compared with the CO molecule, and the Ni adatom acts as an electron bridge linking the charge-transfer from the WSe_2 surface to the HCHO molecule. In the CDD distribution, we find that the electron accumulations are dominantly on the HCHO molecule, the Ni adatom and the Ni−O and Ni−C bonds, which not only support the results from Hirshfeld analysis but also prove the strong orbital interaction in the Ni−O and Ni−C bonds where electron hybridization occurs. Also, the slight electron depletion on the C═O and C−H bonds of the adsorbed HCHO molecule can be found, revealing the geometric distortion on the HCHO molecule after optimization in which the binding force becomes somewhat weakened.

Furthermore, based on the gas adsorption of CO and HCHO onto the pristine WSe_2 monolayer, it is found that the adsorption energy are calculated as −0.51 and −0.57 eV, respectively. That is, the adsorption strength of the Ni-WSe_2 monolayer is about 4.45 and 2.40 times in comparison with the pristine WSe_2 monolayer in terms of adsorbing CO and HCHO molecules. These findings verify the favorable binding force of the Ni adatom upon two gas species that largely enhances the adsorption performance of the WSe_2 monolayer upon them.

3.3. Electronic Properties in Gas Adsorptions. To understand the deformed electronic property of the Ni-WSe_2 monolayer after CO and HCHO adsorptions, the BS of these two systems should be analyzed. Besides, the molecular DOS and orbital DOS in the gas adsorption systems would be helpful to better comprehend the electronic properties of the gas species and the orbital interaction between bonded atoms. For such three purposes, the BS, molecular DOS and orbital DOS of the gas adsorbed systems are exhibited in Figure 4. One should note that the spin and spin down of the gas adsorbed systems are symmetric, indicating their nonmagnetic property for two gas adsorbed systems.

From the BS distributions, it can be seen that the band gaps of the CO and HCHO systems are obtained as 1.320 and 1.343 eV, respectively, which are both reduced in comparison with those of the isolated Ni-WSe_2 system. In other words, the electrical conductivity of the Ni-WTe_2 monolayer would be somewhat increase after adsorptions of CO and HCHO. This bring about the sensing mechanism to explore the Ni-WSe_2 monolayer as a typical gas sensor. Such findings would be further confirmed using the Frontier molecular orbital theory in the next section to explore its sensing potential. From the molecular DOS, it could be found that the states of the isolated gas molecules suffer dramatic deformations after adsorption, which are basically left-shifted and split into several novel small states in their adsorbed phase. These new-formed states, especially the ones near the Fermi level, can contribute largely to the electronic states of the Ni-WSe_2 monolayer, thus deforming its band gap and electrical conductivity.

Moreover, from the orbital DOS of the bonded atoms, we can see that the Ni 3d orbital is highly hybrid with the C 2p orbital of the CO molecule at −6.8, −6.1, −1.4, −0.7, and 1.5 eV, whereas with the C 2p and the O 2p orbital (the state hybridizations are almost at the same states) of the HCHO molecule at −6.9, −6.0, −5.3, −1.7, −0.6, −0.2, and 1.5 eV. These state hybridizations reveal the favorable orbital interaction in the Ni−C and Ni−O bonds for CO and HCHO adsorptions, which demonstrates the formation of covalent bonds in the Ni-WSe_2/gas systems. Besides, in the HCHO system, the overlapped state areas between the Ni 3d and O 2p orbitals are much larger than that between the Ni 3d and the O 2p orbitals, which verifies the stronger binding force of the Ni−O bond in comparison with the Ni−C bond. Such findings about the electronic property clearly illustrate the adsorption performance of the Ni-WSe_2 monolayer upon gas species.

3.4. Gas Sensor Exploration. To further investigate the changed electrical conductivity of the Ni-WSe_2 monolayer after gas adsorptions, we adopt Frontier molecular orbital theory to obtain the highest occupied molecular orbital (HOMO) and the lowest unoccupied molecular orbital (LUMO) of the gas adsorbed system. It is worth mentioning that the energy gap between the HOMO and LUMO is also an important and workable parameter to evaluate the electrical conductivity of the sensing materials.[45] Based on the Frontier molecular orbital theory, the HOMO and LUMO distributions with their energies are portrayed in Figure 5.

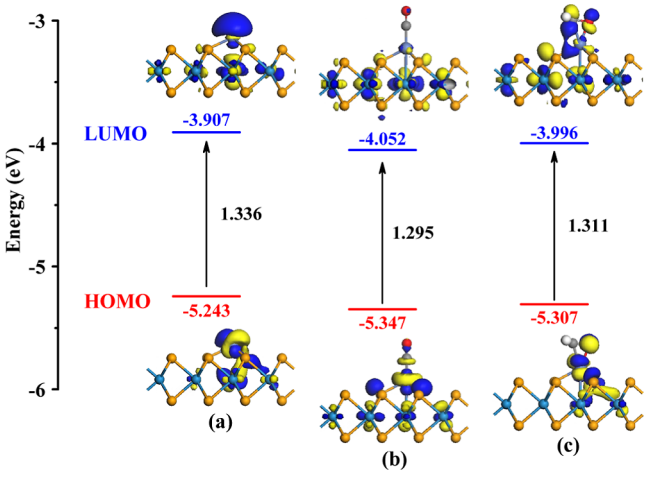

Figure 5. HOMO and LUMO distributions of (a) pure Ni-WSe_2 monolayer and (b,c) CO and HCHO system.

From this figure, one can see that in the Ni-WSe_2 monolayer, the HOMO and LUMO are mainly on the Ni atom, which reflects its strong chemical reactivity and electron mobility in the interactions. Accordingly, the energies for HOMO and LUMO are obtained as −5.243 and −3.907 eV, respectively, with the energy gap calculated to be 1.336 eV. In addition, in the gas adsorbed systems, one can see that the HOMO and LUMO distributions are largely deformed. Specifically, the LUMO distribution on the Ni adatom is largely reduced, while obvious accumulation could be found on the CO and HCHO molecules; in the meanwhile, the HOMO

https://doi.org/10.1021/acsomega.3c06980
ACS Omega 2023, 8, 47067−47074

distribution on the Ni atom is not largely impacted, but there are still remarkable distributions on the CO and HCHO molecules. These HOMO and LUMO distributions reveal the probably orbital interaction between the bonded atoms, indicating the favorable chemical reactions in gas adsorptions.[46] It is worth noting that along with the changed distributions in HOMO and LUMO, their energies are altered to some extent as well. We can find that the energies of HOMO in the CO and HCHO systems are reduced to −4.052 and −3.996 eV, respectively, while the energies of LUMO in such two systems declined to −5.347 and −5.307 eV, respectively. In this regard, the energy gaps in the CO and HCHO systems are calculated to be 1.295 and 1.311 eV, respectively. From the comparison, it could be concluded that the energy gap of the Ni-WSe_2 monolayer would be decreased by 3.07% after CO adsorption and by 1.87% after HCHO adsorption. Such results are basically in agreement with the changing rate of the band gap in the two systems, which are calculated as 3.08% in the CO system and 1.40% in the HCHO system. These findings means the increased electrical conductivity of the Ni-WSe_2 monolayer to different levels after adsorptions of two gas species.[47]

It is well-known that the electrical conductivity (σ) of the sensing material has a relationship with its band gap (energy gap), expressed as[14]

$$\sigma = e^{(-B_g/2kT)} \tag{3}$$

wherein B_g is the band gap (energy gap) of the analyzed system, T is the temperature, and k is the Boltzmann constant (1.38×10^{-23} J/K). Besides, the sensing response (S) of a resistance-type gas sensor can be calculated by[48]

$$S = (\sigma_{gas}^{-1} - \sigma_{pure}^{-1})/\sigma_{pure}^{-1} \tag{4}$$

in which σ_{gas} and σ_{pure} are the electrical conductivity of the gas adsorbed system and isolated sensing material, respectively. On basis of such two equations, the sensing response of Ni-WSe_2 monolayer can be further expressed by

$$S = e^{B_{gg} - B_{gi}/2kT} - 1 \tag{5}$$

in which the B_{gg} is the band gap (energy gap) of the Ni-WSe_2/gas system, while the B_{gi} is the band gap (energy gap) of the isolated Ni-WSe_2 system. Based on eq 5, the sensing response of the Ni-WSe_2 monolayer for detection of CO and HCHO can be calculated as 55.9 and 30.9% using the band gap and as 55.0 and 38.5% using the energy gap. These reveal the desirable sensing performance of the Ni-WSe_2 monolayer as a novel resistance-type gas sensor for CO and HCHO detection in dry-type transformers.

Moreover, it is worth noting that gas adsorptions would also impact the work function (WF) of the sensing material, which provides its potential to be explored as a WF-based gas sensor.[49] Based on our calculations, the WF of the isolated Ni-WSe_2 monolayer and gas adsorbed systems are presented in Figure 6. One can see from this figure that the WF of the Ni-WSe_2 monolayer is obtained as 4.98 eV, while those for the CO and HCHO systems are obtained as 5.12 and 5.09 eV, respectively. That is, the WF of the Ni-WSe_2 monolayer is changed by 2.8% after CO adsorption and 2.2% after HCHO adsorption. However, due to the quite limited changing rate of WF in the gas adsorbed systems in comparison with the pure Ni-WSe_2 monolayer, we assume that it has weak sensing performance to be explored as a WF-based sensor for gas detection.

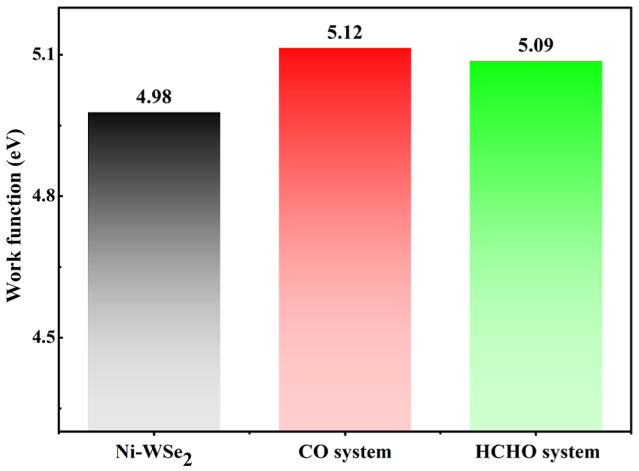

Figure 6. WF of isolated Ni-WSe_2 monolayer and gas adsorbed system.

4. CONCLUSIONS

In this paper, the Ni-WSe_2 monolayer is purposed using first-principles theory to be a novel sensing material to detect CO and HCHO in the dry-type transformers. The main conclusions are as follows:

1 The Ni atom prefers to be chemical stably doped on the T_W site of the WSe_2 surface, with E_b of −4.33 eV, narrowing the band gap of the pristine WSe_2 monolayer instead;
2 Ni-WSe_2 monolayer performs chemisorption upon CO and HCHO, with E_{ad} values of −2.27 and −1.37 eV, respectively.
3 The BS analysis manifests the sensing response of the Ni-WSe_2 monolayer to be 55.9% upon CO and to be 30.9% upon HCHO, uncovering its potential as a resistance-type gas sensor;
4 The WF analysis reveals the limited possibility to explore the Ni-WSe_2 monolayer as a WF-based gas sensor for CO and HCHO detections.

The findings in this work fully elucidate the sensing potential of the Ni-WSe_2 monolayer upon two typical gas species in the dry-type transformers, which is helpful for electrical equipment monitoring using novel nanomaterial-based gas sensor.

AUTHOR INFORMATION

Corresponding Author

Hao Cui − *College of Artificial Intelligence, Southwest University, Chongqing 400715, China;* orcid.org/0000-0002-9410-6345; Email: cuihaocqu@163.com

Authors

Yan Liu − *State Key Laboratory of Power Grid Environmental Protection, China Electric Power Research Institute, Wuhan 430074, China*

Jianben Liu − *State Key Laboratory of Power Grid Environmental Protection, China Electric Power Research Institute, Wuhan 430074, China*

Zhuo Wei − *China Electric Power Research Institute, Wuhan 430074, China*

https://doi.org/10.1021/acsomega.3c06980
ACS Omega 2023, 8, 47067−47074

Tian Yuan − *China Electric Power Research Institute, Wuhan 430074, China;* orcid.org/0000-0003-2230-5318

Complete contact information is available at: https://pubs.acs.org/10.1021/acsomega.3c06980

Notes

The authors declare no competing financial interest.

■ ACKNOWLEDGMENTS

This work was supported by Open Fund of State Key Laboratory of Power Grid Environmental Protection (no. GYW51202301430).

■ REFERENCES

(1) Zhang, Y. L.; Wang, L.; Xiong, L.; Zhao, Y. L.; Yang, Z. K.; Wei, H. E. On-line Temperature Monitoring and State Evaluation System for 10kV Dry-type Transformers. *Electrical Measurement & Instrumentation*, 2012.

(2) Rahimpour, E.; Azizian, D. Analysis of Temperature Distribution in Cast-resin Dry-type Transformers. *Electr. Eng.* **2007**, *89* (4), 301−309.

(3) Eslamian, M.; Vahidi, B.; Eslamian, A. Thermal analysis of cast-resin dry-type transformers. *Energy Convers. Manag.* **2011**, *52* (7), 2479−2488.

(4) Xiong, L.; Zhao, Y.; Yang, Z.; Song, D.; He, W. Temperature rise analysis and calculation of cast resin dry-type transformers. *Gaodianya Jishu* **2013**, *39* (2), 265−271.

(5) Wang, Y.; Feng, C.; Fei, R.; Luo, Y. Thermal-ageing characteristics of dry-type transformer epoxy composite insulation. *High Perform. Polym.* **2020**, *32* (7), 741−752.

(6) Li, Y.; Guan, Y. J.; Li, Y.; Li, T. Y. Calculation of Thermal Performance in Amorphous Core Dry-Type Transformers. *Adv. Mater. Res.* **2014**, *986*−*987*, 1771−1774.

(7) Park, C. Y.; Park, D. W.; Choi, J. S.; Kil, G. S. A Study on PD Detection Methods for Cast-resin Dry-type Transformers. *J. Kor. Inst. Electr. Electron. Mater. Eng.* **2009**, *22* (9), 786−791.

(8) Cui, H.; Zhang, X.; Li, Y.; Chen, D.; Zhang, Y. First-principles insight into Ni-doped InN monolayer as a noxious gases scavenger. *Appl. Surf. Sci.* **2019**, *494*, 859−866.

(9) Zhang, D.; Liu, J.; Jiang, C.; Liu, A.; Xia, B. Quantitative detection of formaldehyde and ammonia gas via metal oxide-modified graphene-based sensor array combining with neural network model. *Sens. Actuators, B* **2017**, *240*, 55−65.

(10) He, Y.; Tao, L.; Li, J.; Wu, M.; Poldorn, P.; Dastan, D.; Abbasi, S.; Nie, S.; Yin, X.; Wang, Q. J. M. T. N. Atomic-level insights into selective adsorption of H2 and CO on SnO2/CoO heterojunctions. *Mater. Today Nano* **2023**, *22*, 100334.

(11) Cui, H.; Zhang, X.; Zhang, J.; Zhang, Y. Nanomaterials-based gas sensors of SF6 decomposed species for evaluating the operation status of high-voltage insulation devices. *High Volt.* **2019**, *4* (4), 242−258.

(12) Tao, L.; Dastan, D.; Wang, W.; Poldorn, P.; Meng, X.; Wu, M.; Zhao, H.; Zhang, H.; Li, L.; An, B. J. A. A. M. Metal-Decorated InN Monolayer Senses N_2 against CO_2. *ACS Appl. Mater. Interfaces* **2023**, *15* (9), 12534−12544.

(13) Keum, D. H.; Cho, S.; Kim, J. H.; Choe, D. H.; Sung, H. J.; Kan, M.; Kang, H.; Hwang, J. Y.; Kim, S. W.; Yang, H.; et al. Bandgap opening in few-layered monoclinic MoTe2. *Nat. Phys.* **2015**, *11* (6), 482−486.

(14) Cui, H.; Guo, Y.; Zhao, Q.; Zhang, G. Pd-doped PtSe2 monolayer with strain-modulated effect for sensing SF6 decomposed species: a first-principles study. *J. Mater. Res. Technol.* **2022**, *18*, 629−636.

(15) Wu, H.; Xia, Y.; Zhang, C.; Xie, S.; Wu, S.; Cui, H. Adsorptions of C5F10O decomposed compounds on the Cu-decorated NiS2 monolayer: a first-principles theory. *Mol. Phys.* **2023**, *121*, No. e2163715.

(16) Yuwen, L.; Xu, F.; Xue, B.; Luo, Z.; Zhang, Q.; Bao, B.; Su, S.; Weng, L.; Huang, W.; Wang, L. General synthesis of noble metal (Au, Ag, Pd, Pt) nanocrystal modified MoS2 nanosheets and the enhanced catalytic activity of Pd-MoS2 for methanol oxidation. *Nanoscale* **2014**, *6* (11), 5762−5769.

(17) Zhao, B.; Li, C. Y.; Liu, L. L.; Zhou, B.; Zhang, Q. K.; Chen, Z. Q.; Tang, Z. Adsorption of gas molecules on Cu impurities embedded monolayer MoS2: A first-principles study. *Appl. Surf. Sci.* **2016**, *382*, 280−287.

(18) Cui, H.; Jia, P.; Peng, X. Adsorption of SO2 and NO2 molecule on intrinsic and Pd-doped HfSe2 monolayer: A first-principles study. *Appl. Surf. Sci.* **2020**, *513*, 145863.

(19) Cui, H.; Zhang, G.; Zhang, X.; Tang, J. Rh-doped MoSe2 as toxic gas scavenger: A first-principles study. *Nanoscale Adv.* **2019**, *2019* (1), 772−780.

(20) Cui, H.; Zhang, X.; Zhang, G.; Tang, J. Pd-doped MoS2 monolayer: A promising candidate for DGA in transformer oil based on DFT method. *Appl. Surf. Sci.* **2019**, *470*, 1035−1042.

(21) Zhang, X.; Wang, J.; Chen, D.; Liu, L. The adsorption performance of harmful gas on Cu doped WS2: A First-principle study. *Mater. Today Commun.* **2021**, *28*, 102488.

(22) Muoi, D.; Hieu, N. N.; Phung, H. T. T.; Phuc, H. V.; Amin, B.; Hoi, B. D.; Hieu, N. V.; Nhan, L. C.; Nguyen, C. V.; Le, P. T. T. Electronic properties of WS2 and WSe2 monolayers with biaxial strain: A first-principles study. *Chem. Phys.* **2019**, *519*, 69−73.

(23) Zhang, D.; Wang, D.; Pan, W.; Tang, M.; Zhang, H. Construction and DFT study of Pd decorated WSe2 nanosheets for highly sensitive CO detection at room temperature. *Sensor. Actuator. B Chem.* **2022**, *360*, 131634.

(24) Xu, L.; Gui, Y.; Li, W.; Li, Q.; Chen, X. Gas-sensing properties of Ptn-doped WSe2 to SF6 decomposition products. *J. Ind. Eng. Chem.* **2021**, *97*, 452−459.

(25) Cui, H.; Yan, C.; Jia, P.; Cao, W. Adsorption and sensing behaviors of SF6 decomposed species on Ni-doped C3N monolayer: A first-principles study. *Appl. Surf. Sci.* **2020**, *512*, 145759.

(26) Zhou, X.; Chu, W.; Zhou, Y.; Sun, W.; Xue, Y. DFT simulation on H2 adsorption over Ni-decorated defective h-BN nanosheets. *Appl. Surf. Sci.* **2018**, *439*, 246−253.

(27) Zhang, D.; Cao, Y.; Yang, Z.; Wu, J. Nanoheterostructure Construction and DFT Study of Ni-Doped In2O3 Nanocubes/WS2 Hexagon Nanosheets for Formaldehyde Sensing at Room Temperature. *ACS Appl. Mater. Interfaces* **2020**, *12* (10), 11979−11989.

(28) Li, P.; Hong, Q.; Wu, T.; Cui, H. SOF2 sensing by Rh-doped PtS2 monolayer for early diagnosis of partial discharge in the SF6 insulation device. *Mol. Phys.* **2021**, *119* (11), No. e1919774.

(29) Yong, Y.; Gao, R.; Yuan, X.; Zhao, Z.; Hu, S.; Kuang, Y. Gas sensing and capturing based on the C7N6 monolayer with and without metal decoration: A first-principles investigation. *Appl. Surf. Sci.* **2022**, *591*, 153129.

(30) Cui, H.; Liu, T.; Zhang, Y.; Zhang, X. Ru-InN Monolayer as a Gas Scavenger to Guard the Operation Status of SF6 Insulation Devices: A First-Principles Theory. *IEEE Sensor. J.* **2019**, *19* (13), 5249−5255.

(31) Tkatchenko, A.; DiStasio, R. A.; Head-Gordon, M.; Scheffler, M. Dispersion-corrected Møller−Plesset second-order perturbation theory. *J. Chem. Phys.* **2009**, *131* (9), 171.

(32) Cui, H.; Liu, Z.; Jia, P. Pd-doped C3N monolayer: A promising low-temperature and high-activity single-atom catalyst for CO oxidation. *Appl. Surf. Sci.* **2021**, *537*, 147881.

(33) Monkhorst, H. J.; Pack, J. D. Special points for Brillouin-zone integrations. *Phys. Rev. B: Condens. Matter Mater. Phys.* **1976**, *13* (12), 5188−5192.

(34) Ma, D.; Ju, W.; Li, T.; Zhang, X.; He, C.; Ma, B.; Lu, Z.; Yang, Z. The adsorption of CO and NO on the MoS2 monolayer doped with Au, Pt, Pd, or Ni: A first-principles study. *Appl. Surf. Sci.* **2016**, *383*, 98−105.

(35) Zhang, D.; Li, Q.; Li, P.; Pang, M.; Luo, Y. Fabrication of Pd-decorated MoSe 2 nanoflowers and density functional theory

simulation toward ammonia sensing. *IEEE Electron Device Lett.* **2019**, *40* (4), 616−619.
(36) Fan, Y.; Zhang, J.; Qiu, Y.; Zhu, J.; Zhang, Y.; Hu, G. A DFT study of transition metal (Fe, Co, Ni, Cu, Ag, Au, Rh, Pd, Pt and Ir)-embedded monolayer MoS2 for gas adsorption. *Comput. Mater. Sci.* **2017**, *138*, 255−266.
(37) Zhai, S.; Jiang, X.; Wu, D.; Chen, L.; Su, Y.; Cui, H.; Wu, F. Single Rh atom decorated pristine and S-defected PdS2 monolayer for sensing thermal runaway gases in a lithium-ion battery: A first-principles study. *Surface. Interfac.* **2023**, *37*, 102735.
(38) Pyykkö, P.; Atsumi, M. Molecular single-bond covalent radii for elements 1−118. *Chemistry* **2009**, *15* (1), 186−197.
(39) Yang, A.; Chu, J.; Li, W.; Wang, D.; Yang, X.; Lan, T.; Wang, X.; Rong, M.; Koratkar, N. Short period sinusoidal thermal modulation for quantitative identification of gas species. *Nanoscale* **2020**, *12* (1), 220−229.
(40) Wang, X. H.; Wang, D. W.; Yang, A. J.; Koratkar, N.; Chu, J. F.; Lv, P. L.; Rong, M. Z. Effects of adatom and gas molecule adsorption on the physical properties of tellurene: a first principles investigation. *Phys. Chem. Chem. Phys.* **2018**, *20* (6), 4058−4066.
(41) Chaurasiya, R.; Dixit, A.; Pandey, R. Strain-mediated stability and electronic properties of WS2, Janus WSSe and WSe2 monolayers. *Superlattice. Microst.* **2018**, *122*, 268−279.
(42) Ma, D.; Ju, W.; Li, T.; Zhang, X.; He, C.; Ma, B.; Tang, Y.; Lu, Z.; Yang, Z. Modulating electronic, magnetic and chemical properties of MoS2 monolayer sheets by substitutional doping with transition metals. *Appl. Surf. Sci.* **2016**, *364*, 181−189.
(43) Rao, G. S.; Hussain, T.; Islam, M. S.; Sagynbaeva, M.; Gupta, D.; Panigrahi, P.; Ahuja, R. Adsorption mechanism of graphene-like ZnO monolayer towards CO2 molecules: enhanced CO2 capture. *Nanotechnology* **2016**, *27* (1), 015502.
(44) Allian, A. D.; Takanabe, K.; Fujdala, K. L.; Hao, X.; Truex, T. J.; Cai, J.; Buda, C.; Neurock, M.; Iglesia, E. Chemisorption of CO and mechanism of CO oxidation on supported platinum nanoclusters. *J. Am. Chem. Soc.* **2011**, *133* (12), 4498−4517.
(45) Cui, H.; Jia, P.; Peng, X.; Hu, X. Geometric, Electronic and Optical Properties of Pt-Doped C3N Monolayer Upon NOx Adsorption: A DFT Study. *IEEE Sensor. J.* **2021**, *21* (3), 3602−3608.
(46) Chu, J.; Li, W.; Yang, X.; Wu, Y.; Wang, D.; Yang, A.; Yuan, H.; Wang, X.; Li, Y.; Rong, M. Identification of gas mixtures via sensor array combining with neural networks. *Sensor. Actuator. B Chem.* **2021**, *329*, 129090.
(47) Wang, Y.; Gui, Y.; Ji, C.; Tang, C.; Zhou, Q.; Li, J.; Zhang, X. Adsorption of SF6 decomposition components on Pt3-TiO2 (1 0 1) surface: A DFT study. *Appl. Surf. Sci.* **2018**, *459*, 242−248.
(48) Verlag, S. Semiconductor Physical Electronics. *Semiconductor Physical Electronics*; Springer, 2006; *28* (3), pp 363−364.
(49) Cui, H.; Feng, Z.; Wang, W.; Peng, X.; Hu, J. Adsorption Behavior of Pd-Doped PtS_2 Monolayer Upon SF_6 Decomposed Species and the Effect of Applied Electric Field. *IEEE Sensor. J.* **2022**, *22* (7), 6764−6771.

https://doi.org/10.1021/acsomega.3c06980
ACS Omega 2023, 8, 47067−47074